GCCAGCTAGAGTAACTGTTACCCC-3′ and 5′-AGTCAC-TTGCCTTGAGCACAGCAC-3′. The amplified products were cloned into a p3T vector for sequencing.

Deduced amino acid sequences, were aligned and phylogenetic trees and homology analyses were done using BLAST (blast.genome.jp), CLC Free Workbench ver 3.2.3 (CLC Bio, Aarhus, Denmark), and Genetyx ver 9.0 (Genetyx Co., Tokyo, Japan).

Recombinant protein

The ORFs of BmDJ-1 were amplified by PCR using PfuTurbo DNA polymerase and primers 5′-AGCAAGTCTGCGTTAGT-GAT-3′ and 5′-TTAGTACTGCGAGATTAACA-3′. Products were cloned into a prokaryotic expression vector pTrcHis-TOPO with a TOPO TA cloning kit (Invitrogen) and expressed in *E. coli* as fusion proteins with N-terminal Xpress tags. The nucleotide sequence was confirmed by sequencing. Recombinant BmDJ-1 expressed in *E. coli* was purified with HIS-Select spin columns (Sigma, St. Louis, MO, USA) according to methods described previously [27]. A recombinant β-galactosidase (LacZ) fragment tagged with X-press included in the TOPO TA cloning kit was used as a negative control.

Immunology

The antibody for immunoblotting was raised in Japanese white rabbits by subcutaneous injection of the recombinant BmDJ-1 and Ribi adjuvant system (Corixa Co., Hamilton, MT, USA) mixture. The serum was stored at −80°C.

Immunoblotting

To identify the presence of BmDJ-1 in different tissues and cells, protein samples (5 μg) were separated on SDS-PAGE, transferred to nitrocellulose membranes using the method of Towbin *et al.* [28], and immunoblotted using rabbit anti-BmDJ-1 antibody and goat anti-rabbit IgG-conjugated horseradish peroxidase (HRP). The membranes were developed using a chemiluminescent substrate (Pierce, Rockford, IL, USA).

The tissue distribution of BmDJ-1 was determined for the midgut, fatbody, Malpighian tubule, testis, and ovary from day 0 fifth instar larvae, pupae, and adults. Each tissue sample was run on the same gel, which was also loaded with 20 ng of recombinant Xpress-tagged BmDJ-1. The distribution of BmDJ-1 from first to fifth instar larvae, pupae and adult on the whole body and brain of larvae, pupae and adults were also determined. All tissues were homogenized in RIPA lysis buffer composed of 50 mM Tris-HCl, pH 7.5, 150 mM NaCl, 1% Nonidet P40, 0.5% sodium deoxycholate, 0.1% SDS, and a cocktail of protease inhibitors (Sigma), followed by centrifugation at 10,000× g for 15 min.

The protein concentration was determined by a Bradford assay kit (Pierce). Samples of supernatant (5 μg of protein) were separated by SDS-PAGE, transferred to nitrocellulose membranes, and immunoblotted with anti-BmDJ-1 antibody following the procedure described above.

Specificity of antibody against BmDJ-1

We examined the specificity of antibody against BmDJ-1 using following samples: 0.25 or 0.5 μg recombinant BmDJ-1 protein with xpress tag, 1 μg recombinant CBP protein with GST tag [21], 10 μg HEK293 cell lysate, BmN4 cell lysate and 10 μg larva brain lysate.

Northern blot analysis

Total RNA derived from the ovaries of day 4 fifth instar larvae were used. Total RNA (12 μg) was separated on a 1.5% agarose-6% formaldehyde gel and transferred to a nylon membrane. DIG-labeled probes were synthesized using the PCR DIG probe synthesis kit (Roche Diagnostics, Mannheim, Germany) according to the supplier's instructions with the primers 5′-CATTT-GTGCTGCTTCCATAGCGTT-3′ and 5′-CATTCCCTTTT-CGACTTGATCGGC-3′. After pre-hybridization, the membranes were hybridized with the DIG-labeled probes at 54°C overnight. The specific reaction was visualized on Kodak X-OMAT AR X-ray films by the DIG chemiluminescence detection kit (Roche Diagnostics).

RT-PCR

Total RNA derived from the brain, midgut, fatbody, Malpighian tubule, testis, ovary, and hemocyte of day 4 fifth instar larvae was DNase-treated and processed for cDNA synthesis using oligo(dT)12–18 primers and SuperScript II reverse transcriptase (Invitrogen). cDNA was amplified by PCR using Taq DNA polymerase (Qiagen) and the primers 5′-CATTTGTGCTG-CTTCCATAGCGTT-3′ and 5′-CATTCCCTTTTCGACTT-GATCGGC-3′. Amplification was carried out for 30 cycles of denaturing for 40 s at 94°C, annealing for 40 s at 50°C and extension for 90 s at 72°C. Amplified PCR products were separated by agarose gel, stained with ethidium bromide, and visualized under UV light.

Transfer plasmid and generation of recombinant virus

The ORF sequence of BmDJ-1 was amplified by PCR from brain cDNA as described above, with the primers 5′-GGG-GTACCCCATGAGCAAGTCTGCGTTAGTGAT-3′ and 5′-GGAATTCCAATATTAGTACTGCGAGATTAAC-3′. The amplified region was digested with EcoRI and KpnI and cloned into the baculovirus transfer pBK283 vector. Blank pBK283 vector was used as a control. For generating recombinant BmNPV, we used a Bom-EX kit (NOSAN) according to the supplier's instructions. The recombinant BmNPV nucleotide sequence was confirmed by sequencing using the primers 5′-ACTGTCGACAAGCTCTGTCC-3′ and 5′-ACAACGCACA-GAATCTAACGC-3′. Purified recombinant virus was titrated by plaque assay, and high titer stocks (2×10^7 pfu/ml) were used for infecting larvae.

Determination of LD_{50} of day 4 fifth instar larvae by ROT stimulation

To determine the LD_{50} of day 3 fifth instar larvae by ROT (Sigma) stimulation, we injected ROT intrahemocoelically to larvae weighing 3.5 to 4.0 g using a disposable syringe (Terumo, Tokyo, Japan) with a 30G needle. ROT was dissolved in DMSO (prepared immediately before use and stored in the dark) at 0, 1.25, 2.5, 5.0, 10, 20, 40, and 80 μg/g and injected into larvae in a volume of 10 μl/g body weight. The number of dead silkworms after 24 h was counted and the mortality rate (%) = (X/Y)×100 was calculated, where X = dead larvae in the group and Y = total larvae in the group. The mortality rates were analyzed with Probit analyses [29] using the Probit Analysis option in the SAS 8.2 software package (SAS Institute Japan Ltd., Tokyo, Japan) to calculate the LD_{50}.

Overexpression of BmDJ-1 to larvae and exposure to ROT oxidative stimuli

A 50 μl aliquot of BmNPV-BmDJ-1 or BmNPV-blank-vector (1×10^5 pfu/larva) was injected intrahemocoelically into day 0 fifth instar larvae using a disposable syringe (Terumo) with a 30G needle. Blank-vector recombinant virus was injected as a control.

After rearing for 4 days on an artificial diet, larvae were examined for overexpression of BmDJ-1 to assess protection from oxidative stress due to ROT.

Virus-derived BmDJ-1 expression level was measured in the dissected fatbodies of several insects after 1 day (24 h) and 4 days (day 3 fifth instar) by RT-PCR with the primers 5′-ACTGTCGACAAGCTCTGTCC-3′ and 5′-ACAACGCACAGAATCTAACGC-3′.

Virus-derived BmDJ-1 expression level was measured in the dissected fatbodies of several insects after 4 days (day 3 fifth instar) by immunoblotting.

We surmised the ROT dose that would be most effective in the experimental model with exogenous BmDJ-1 based on a report of the administration of exogenous DJ-1 [30].

ROT, prepared at 20 μg/g (LD_{70}), was injected to three groups of 10 to 20 larvae in a volume of 10 μl/g body weight. The number of dead silkworms after 24 h was counted and the mortality rate (%) was calculated.

Data were analyzed with the multiple comparison test followed by the Cochran-Armitage test for dose-response relationship and Steel's (non-parametric) multiple comparison test. $P<0.05$ was considered significant. All statistical analyses were carried out using SAS system 8.2 software. Three trials were performed in each experiment.

BmN4 cells treated with ROT, two-dimensional (2D) gel electrophoresis, and detection of BmDJ-1

BmN4 cells (2×10^6) were grown on 6-well Falcon plates (BD Biosciences, Franklin Lakes, NJ, USA) and washed twice with PBS followed by 3 h of treatment with TC-100 medium containing ROT (50 μM) dissolved in 0.1% DMSO or 0.1% DMSO as a control in the dark. To prepare total protein extracts for two-dimensional (2D) gel electrophoretic analysis, the cells were sonicated in rehydration buffer comprising 8 M urea, 2% CHAPS, 0.5% carrier ampholytes at pH 3–10, 20 mM dithiothreitol, 0.002% bromophenol blue, and a cocktail of protease inhibitors. Urea-soluble proteins were separated by isoelectric focusing (IEF) using the ZOOM IPGRunner system loaded with an immobilized pH 3–10 gradient strip (Invitrogen), as described previously [16]. After the first dimension of IEF, the protein was separated in the second dimension on a 4–12% NuPAGE polyacrylamide gel (Invitrogen). For detection of BmDJ-1, the gel was transferred to a polyvinylidene difluoride (PVDF) membrane for immunoblotting.

All incubation steps were carried out at 25°C in the dark. Three trials were performed for each experiment.

Collection of samples and measurement of NO levels

Hemolymph (250 μl) was collected from day 0 fifth instar larvae, pupae and adults, or from medium to measure the concentration of NO. To remove proteins, samples were mixed with methanol (2:1 by volume), followed by centrifugation at 10,000× *g* for 20 min, and NO levels in the supernatants were measured using an NOx analyzer (ENO-20; Eicom, Kyoto, Japan), according to the manual.

BmN4 cell treatment with ISDN and detection of BmDJ-1

BmN4 cells (2×10^6) were grown on 6-well Falcon plates (BD Biosciences) and washed twice with PBS followed by 16 h of treatment with TC-100 medium containing 100 μM of isosorbide dinitrate (ISDN; prepared immediately prior to use and kept in the dark) dissolved in 0.1% ethanol or with 0.1% ethanol alone as a control. Total protein extracts were prepared for immunoblotting and culture medium was prepared for NO analysis. Statistical analysis was performed using Student's *t*-test. $P<0.05$ was considered significant. All statistical analyses were carried out using SAS system 8.2 software. Three trials were performed for each experiment.

Supporting Information

Figure S1 SDS-PAGE and CBB staining of figure 4. A. AWhole body homogenates from day 0 larvae of the first (lane 1), second (lane 2), third (lane 3), fourth (lane 4), and fifth (lane 5) instars, the pupae (lane 6), and the adult (lane 7). B, Brain of the fifth instar larvae (lane 8), pupae (lane 9), and adults (lane 10). C. a, midgut; b, fatbody; c, Malpighian tubule; d, testis; and e, ovary were isolated from day 0 to 12 fifth instar larvae (lanes 1 to 13), from day 0, 1, 3, 4, 7 and 8 pupae (lanes 14 to 19), and from day 0 adults (lane 20). No samples were loaded in panel a, lanes 17, 18, 19, 20; panel c, lane 16; and panel e, lane 13.
(TIFF)

Figure S2 SDS-PAGE and CBB staining of figure 7B. Non-infected control (day 3 fifth instar larvae)from experiments 1 (lane 1), 2 (lane 2) and 3 (lane 3); infected by recombinant virus from experiments 1 (lane 4), 2 (lane 5), 3 (lane 6); and blank virus after 4 days infection from experiments 1 (lane 7), 2 (lane 8), 3 (lane 9).
(TIFF)

Figure S3 SDS-PAGE and CBB staining of figure 8C. Experiment 1 of control (lane 1), experiment 2 of control (lane 2), experiment 3 of control (lane 3), experiment 1 of ISDN treatment (lane 4), experiment 2 of ISDN treatment (lane 5), and experiment 3 of ISDN treatment (lane 6).
(TIFF)

Acknowledgments

We are indebted to Dr. Taro Tamaki for critical reading of the manuscript, Dr. Yuki Ogasawara for advice on the oxidative stress experiment, Dr. Kikuo Iwabuchi for advice on cell culture, and Ms. Mai Ikeda, Ms. Hiroko Nakano and Ms. Yukiko Senoh for technical assistance.

Author Contributions

Conceived and designed the experiments: HT JS. Performed the experiments: HT HO SK KY. Analyzed the data: TS KM. Contributed reagents/materials/analysis tools: YB RS. Wrote the paper: HT. Measurement of NO levels: RIN.

References

1. Bandyopadhyay S, Cookson MR (2004) Evolutionary and functional relationships within the DJ1 superfamily. BMC Evol Biol 4: 1–9.
2. Costa CA (2007) DJ-1: a newcomer in Parkinson's disease pathology. Curr Mol Med 7: 650–657.
3. Kinumi T, Kimata J, Taira T, Ariga H, Nikia E (2004) Cysteine-106 of DJ-1 is the most sensitive cysteine residue to hydrogen peroxide-mediated oxidation in vivo in human umbilical vein endothelial cells. Biochem Biophys Res Commun 317: 722–728.
4. Bové J, Prou D, Perier C, Przedborski S (2005) Toxin-induced models of Parkinson's disease. NeuroRx 2: 484–494.
5. Terzioglu M, Galter D (2008) Parkinson's disease: genetic versus toxin-induced rodent models. FEBS J 275: 1384–1391.
6. Panov A, Dikalov S, Shalbuyeva N, Taylor G, Sherer T, et al. (2005) Rotenone model of Parkinson disease: multiple brain mitochondria dysfunctions after short term systemic rotenone intoxication. J Biol Chem 280: 42026–42035.

7. Menzies FM, Yenisetti SC, Min KT (2005) Roles of Drosophila DJ-1 in survival of dopaminergic neurons and oxidative stress. Curr Biol 15: 1578–1582.
8. Olzmann JA, Brown K, Wilkinson KD, Rees HD, Huai Q, et al. (2004) Familial Parkinson's disease-associated L166P mutation disrupts DJ-1 protein folding and function. J Biol Chem 279: 8506–8515.
9. Tao X, Tong L (2003) Crystal structure of human DJ-1, a protein associated with early onset Parkinson's disease. J Biol Chem 278: 31372–31379.
10. Anderson PC, Daggett V (2008) Molecular basis for the structural instability of human DJ-1 induced by the L166P mutation associated with Parkinson's disease. Biochemistry 47: 9380–9393.
11. Blackinton J, Lakshminarasimhan M, Thomas KJ, Ahmad R, Greggio E, et al. (2009) Formation of a stabilized cysteine sulfinic acid is critical for the mitochondrial function of the parkinsonism protein DJ-1. J Biol Chem 284: 6476–6485.
12. Meulener MC, Xu K, Thomson L, Ischiropoulos H, Bonini NM (2004) Mutational analysis of DJ-1 in Drosophila implicates functional inactivation by oxidative damage and aging. Proc Natl Acad Sci USA 103: 12517–12522.
13. Mita K, Kasahara M, Sasaki S, Nagayasu Y, Yamada T, et al. (2004) The genome sequence of silkworm, *Bombyx mori*. DNA Res 11: 27–35.
14. Ohnishi A, Hull JJ, Matsumoto S (2006) Targeted disruption of genes in the *Bombyx mori* sex pheromone biosynthetic pathway. Proc Natl Acad Sci USA 103: 4398–4403.
15. Tomita M, Munetsuna H, Sato T, Adachi T, Hino R, et al. (2003) Transgenic silkworms produce recombinant human type III procollagen in cocoons. Nat Biotechnol 21: 52–56.
16. Xia Q, Zhou Z, Lu C, Cheng D, Dai F, et al. (2004) A draft sequence for the genome of the domesticated silkworm (*Bombyx mori*). Science 306: 1937–1940.
17. Xia Q, Cheng D, Duan J, Wang G, Cheng T, et al. (2007) Microarray-based gene expression profiles in multiple tissues of the domesticated silkworm, *Bombyx mori*. Genome Biol 8: R162.
18. Kozak M (1984) Compilation and analysis of sequences upstream from the translational start site in eukaryotic mRNAs. Nucleic Acids Res 12: 857–872.
19. Pedersen AG, Nielsen H (1997) Neural network prediction of translation initiation sites in eukaryotes: perspectives for EST and genome analysis. Proc Int Conf Intell Syst Mol Biol 5: 226–233.
20. Yamamoto K, Narukawa J, Kadono-Okuda K, Nohata J, Sasanuma M, et al. (2006) Construction of a single nucleotide polymorphism linkage map for the silkworm, *Bombyx mori*, based on bacterial artificial chromosome end sequences. Genetics 173: 151–161.
21. Tabunoki H, Sugiyama H, Tanaka Y, Fujii H, Banno Y, et al. (2002) Isolation, characterization, and cDNA sequence of a carotenoid binding protein from the silk gland of *Bombyx mori* larvae. J Biol Chem 277: 32133–32140.
22. Meulener M, Whitworth A J, Armstrong-Gold CE, Rizzu P, Heutink P, et al. (2007) Drosophila DJ-1 mutants are selectively sensitive to environmental toxins associated with Parkinson's disease. Curr Biol 15: 1572–1577.
23. Maeda S, Kawai T, Obinata M, Fujiwara H, Horiuchi T, et al. (1985) Production of human alpha-interferon in silkworm using a baculovirus vector. Nature 315: 592–594.
24. Choi SK, Choi HK, Kadono-Okuda K, Taniai K, Kato Y, et al. (1995) Occurrence of novel types of nitric oxide synthase in the silkworm, *Bombyx mori*. Biochem Biophys Res Commun 207: 452–459.
25. Inoue M, Sato EF, Nishikawa M, Hiramoto K, Kashiwagi A, et al. (2004) Free radical theory of apoptosis and metamorphosis. Redox Rep 9: 237–247. Review.
26. Fan J, Ren H, Jia N, Fei E, Zhou T, et al. (2008) DJ-1 decreases Bax expression through repressing p53 transcriptional activity. J Biol Chem 283: 4022–4030.
27. Tabunoki H, Shimada T, Banno Y, Sato R, Kajiwara H, et al. (2008) Identification of *Bombyx mori* 14-3-3 orthologs and the interactor Hsp60. Neurosci Res 61: 271–280.
28. Towbin H, Staehelin J, Gordon J (1979) Electrophoretic transfer of proteins from polyacrylamide gels to nitrocellulose sheets: procedure and some applications. Proc Natl Acad Sci USA 76: 4350–4354.
29. Finny DJ (1947) Probit Analysis: A Statistical Treatment of the Sigmoid Response Curve. Cambridge, NY: Cambridge University Press. 20 p.
30. Inden M, Taira T, Kitamura Y, Yanagida T, Tsuchiya D, et al. (2006) PARK7 DJ-1 protects against degeneration of nigral dopaminergic neurons in Parkinson's disease rat model. Neurobiol Dis 24: 144–158.

BioData Mining

RESEARCH Open Access

Comprehensive analysis of human microRNA target networks

Jun-ichi Satoh* and Hiroko Tabunoki

* Correspondence: satoj@my-pharm.ac.jp
Department of Bioinformatics and Molecular Neuropathology, Meiji Pharmaceutical University, 2-522-1 Noshio, Kiyose, Tokyo 204-8588, Japan

Abstract

Background: MicroRNAs (miRNAs) mediate posttranscriptional regulation of protein-coding genes by binding to the 3' untranslated region of target mRNAs, leading to translational inhibition, mRNA destabilization or degradation, depending on the degree of sequence complementarity. In general, a single miRNA concurrently downregulates hundreds of target mRNAs. Thus, miRNAs play a key role in fine-tuning of diverse cellular functions, such as development, differentiation, proliferation, apoptosis and metabolism. However, it remains to be fully elucidated whether a set of miRNA target genes regulated by an individual miRNA in the whole human microRNAome generally constitute the biological network of functionally-associated molecules or simply reflect a random set of functionally-independent genes.

Methods: The complete set of human miRNAs was downloaded from miRBase Release 16. We explored target genes of individual miRNA by using the Diana-microT 3.0 target prediction program, and selected the genes with the miTG score ≧ 20 as the set of highly reliable targets. Then, Entrez Gene IDs of miRNA target genes were uploaded onto KeyMolnet, a tool for analyzing molecular interactions on the comprehensive knowledgebase by the neighboring network-search algorithm. The generated network, compared side by side with human canonical networks of the KeyMolnet library, composed of 430 pathways, 885 diseases, and 208 pathological events, enabled us to identify the canonical network with the most significant relevance to the extracted network.

Results: Among 1,223 human miRNAs examined, Diana-microT 3.0 predicted reliable targets from 273 miRNAs. Among them, KeyMolnet successfully extracted molecular networks from 232 miRNAs. The most relevant pathway is transcriptional regulation by transcription factors RB/E2F, the disease is adult T cell lymphoma/leukemia, and the pathological event is cancer.

Conclusion: The predicted targets derived from approximately 20% of all human miRNAs constructed biologically meaningful molecular networks, supporting the view that a set of miRNA targets regulated by a single miRNA generally constitute the biological network of functionally-associated molecules in human cells.

Introduction

MicroRNAs (miRNAs) are a class of endogenous small noncoding RNAs conserved through the evolution. They mediate posttranscriptional regulation of protein-coding genes by binding to the 3' untranslated region (3'UTR) of target mRNAs, leading to translational inhibition, mRNA destabilization or degradation, depending on the degree of sequence complementarity [1]. During the biogenesis of miRNAs, the primary miRNAs (pri-miRNAs) are transcribed from the intra- and inter-genetic regions of the genome by RNA polymerase II, followed by processing by the RNase III enzyme Drosha into pre-miRNAs. After nuclear export, they are cleaved by the RNase III enzyme Dicer into mature miRNAs consisting of approximately 22 nucleotides. Finally, a single-stranded miRNA is loaded onto the RNA-induced silencing complex (RISC), where the seed sequence located at positions 2 to 8 from the 5' end of the miRNA plays a pivotal role in recognition of the target mRNA [2]. At present, more than one thousand of human miRNAs are registered in miRBase Release 16 http://www.mirbase.org. The 3'UTR of a single mRNA is often targeted by several different miRNAs, while a single miRNA concurrently reduces the production of hundreds of target proteins [3]. Consequently, the whole miRNA system (microRNAome) regulate greater than 60% of all protein-coding genes in a human cell [4]. By targeting multiple transcripts and affecting expression of numerous proteins, miRNAs play a key role in fine-tuning of diverse cellular functions, such as development, differentiation, proliferation, apoptosis and metabolism. Therefore, aberrant regulation of miRNA expression is deeply involved in pathological events that mediate cancers [5] and neurodegenerative disorders [6].

Recent advances in systems biology have made major breakthroughs by illustrating the cell-wide map of complex molecular interactions with the aid of the literature-based knowledgebase of molecular pathways [7]. The logically arranged molecular networks construct the whole system characterized by robustness, which maintains the proper function of the system in the face of genetic and environmental perturbations [8]. In the scale-free molecular network, targeted disruption of limited numbers of critical components designated hubs, on which the biologically important molecular interactions concentrate, efficiently disturbs the whole cellular function by destabilizing the network [9]. Therefore, the identification of the hub in the molecular network constructed by target genes of a particular miRNA helps us to understand biological and pathological roles of individual miRNAs. Recently, Hsu et al. studied the human microRNA-regulated protein-protein interaction (PPI) network by utilizing the Human Protein Reference Database (HPRD) and the miRNA target prediction program TargetScan [10]. They found that an individual miRNA often targets the hub gene of the PPI network, although they did not attempt to characterize relevant pathways, diseases, and pathological events regulated by miRNA target genes.

At present, the question remains to be fully elucidated whether a set of miRNA target genes regulated by an individual miRNA in the whole human microRNAome generally constitute the biological network of functionally-associated molecules or simply reflect a random set of functionally-independent genes. To address this question, we attempted to characterize molecular networks of target genes of all human miRNAs by using KeyMolnet, a bioinformatics tool for analyzing molecular interactions on the comprehensive knowledgebase.

Materials and methods

MicroRNA Target Prediction

The complete list of 1,223 human miRNAs was downloaded from miRBase Release 16 http://www.mirbase.org. We searched the target genes of individual miRNA on the Diana-microT 3.0 target prediction program (diana.cslab.ece.ntua.gr/microT), which was selected because of the highest ratio of correctly predicted targets over other prediction tools [11]. Diana-microT 3.0 calculates the miRNA-targeted gene (miTG) score that reflects the weighted sum of the scores of all conserved and non-conserved miRNA recognition elements (MRE) on the 3'UTR of the target mRNA. The miTG score correlates well with fold changes in suppression of protein expression [11]. To optimize the parameter of miRNA-target interaction, we considered the target genes with a cutoff of the miTG score equal to or larger than 20 as the highly reliable targets, because we found that the targets with the miTG score < 20 exhibited the significantly lower precision score, an indicator of correctness in predicted interactions [11], compared with those having the score ≧ 20 ($p = 2.78E-08$ by Mann-Whitney's U-test).

Molecular Network Analysis

Ensembl Gene IDs of target genes retrieved by Diana-microT 3.0 were converted into the corresponding Entrez Gene IDs by using the DAVID Bioinformatics Resources 6.7 program http://david.abcc.ncifcrf.gov[12], where non-annotated IDs were deleted. Then, Entrez Gene IDs of miRNA target genes were uploaded onto KeyMolnet.

KeyMolnet is a tool for analyzing molecular interactions on the literature-based knowledgebase that contains the contents on 123,000 molecular relationships among human genes and proteins, small molecules, diseases, pathways and drugs, established by the Institute of Medicinal Molecular Design (IMMD) (Tokyo, Japan) [13-15]. The core contents are collected from selected review articles and textbooks with the highest reliability, regularly updated and carefully curated by a team of expert biologists. KeyMolnet contains a panel of human canonical networks constructed by core contents in the KeyMolnet library. They represent the gold standard of the networks, composed of 430 pathways, 885 diseases, and 208 pathological events. Detailed information on all the contents is available from IMMD http://www.immd.co.jp/en/keymolnet/index.html upon request.

We utilized the neighboring network-search algorithm that selects the set of miRNA target genes as starting points to generate the network around starting points within one path, composed of all kinds of molecular interactions, including direct activation/inactivation, transcriptional activation/repression, and the complex formation. By uploading the list of Entrez Gene IDs onto KeyMolnet, it automatically provides corresponding molecules and a minimum set of intervening molecules as a node on networks. The generated network was compared side by side with human canonical networks described above. The algorithm that counts the number of overlapping molecules and/or molecular relations between the extracted network and the canonical network identifies the canonical network showing the most statistically significant contribution to the extracted network. This algorithm is essentially based on that of the GO::TermFinder [16]. The significance in the similarity between the extracted network and the canonical network is scored following the formula, where O = the number of overlapping molecules and molecular relations for the pathway or overlapping molecules alone for the disease and the pathological event between the extracted network and the canonical network, V = the number of molecules

and/or molecular relations located in the extracted network, C = the number of molecules and/or molecular relations located in the canonical network, T = the number of total molecules and/or molecular relations of KeyMolnet, currently composed of approximately 15,700 molecules and 123,000 molecular relations, and the × = the sigma variable that defines coincidence.

$$\text{Score} = -\log_2(\text{Score (p)}) \qquad \text{Score (p)} = \sum_{x=O}^{Min(C,V)} f(x) \qquad \text{f(x)} = {}_{C}C_{x} \cdot {}_{T-C}C_{V-x}/{}_{T}C_{V} \quad (1)$$

Results

Molecular Network of MicroRNA Target Genes

Among 1,223 human miRNAs examined, Diana-microT 3.0 predicted the targets from 532 miRNAs (43.5%). Among the 532 miRNAs, 273 miRNAs contained a set of highly reliable targets showing the miTG score ≧ 20. Among 273 miRNAs having reliable targets, KeyMolnet successfully extracted molecular networks from 232 miRNAs. They are comprised of 19% of total human miRNAs (microRNAome). Then, the generated network was compared side by side with human canonical networks of the KeyMolnet library, composed of 430 pathways, 885 diseases, and 208 pathological events. We found that not all 232 miRNAs contained entire categories of canonical networks because several miRNAs comprised relatively small numbers of targets. See Additional file 1 for all the information on 232 miRNAs and their target networks. When top three pathways, diseases, and pathological events were individually totalized, the most relevant pathway is 'transcriptional regulation by RB/E2F' (n = 39; 6.8% of total), followed by 'TGF-beta family signaling pathway' (n = 32; 5.6%) and 'transcriptional regulation by POU domain factor' (n = 24; 4.2%), the most relevant disease is 'adult T cell lymphoma/leukemia' (n = 68; 12.1%), followed by 'chronic myelogenous leukemia' (n = 65; 11.5%) and 'hepatocellular carcinoma' (n = 51; 9.1%), and the most relevant pathological event is 'cancer' (n = 97; 24.7%), followed by 'adipogenesis' (n = 46; 11.7%) and 'metastasis' (n = 36; 9.2%) (Figure 1 and Additional file 1).

Next, we identified the large-scale miRNA target networks by uploading targets greater than 100 per individual miRNA onto KeyMolnet (Table 1). Fifty-two miRNAs that construct such a large-scale miRNA target network include let-7, miR-9, 17, 19, 20, 26, 27, 29, 30, 32, 92, 93, 96, 98, 101, 106b, 124, 137, 147, 153, 218, 372, 429, 495, 506, 519, 520, 603, and their closely-related family members. The targets of these miRNAs established highly complex molecular networks, in which the pathways of 'transcriptional regulation by RB/E2F', 'transcriptional regulation by Ets-domain family', and 'transcriptional regulation by p53', the diseases of 'chronic myelogenous leukemia' and 'viral myocarditis', and the pathological event of 'cancer' were notably accumulated (Table 1). Importantly, distinct members belonging to the same miRNA family, for example, five miR-30 family members ranging from miR-30a to miR-30e constructed a virtually identical molecular network (Table 1).

Biological Implications of MicroRNA Target Networks

As described above, the present observations indicated that a set of miRNA target genes regulated by an individual miRNA generally constitute the biological network of

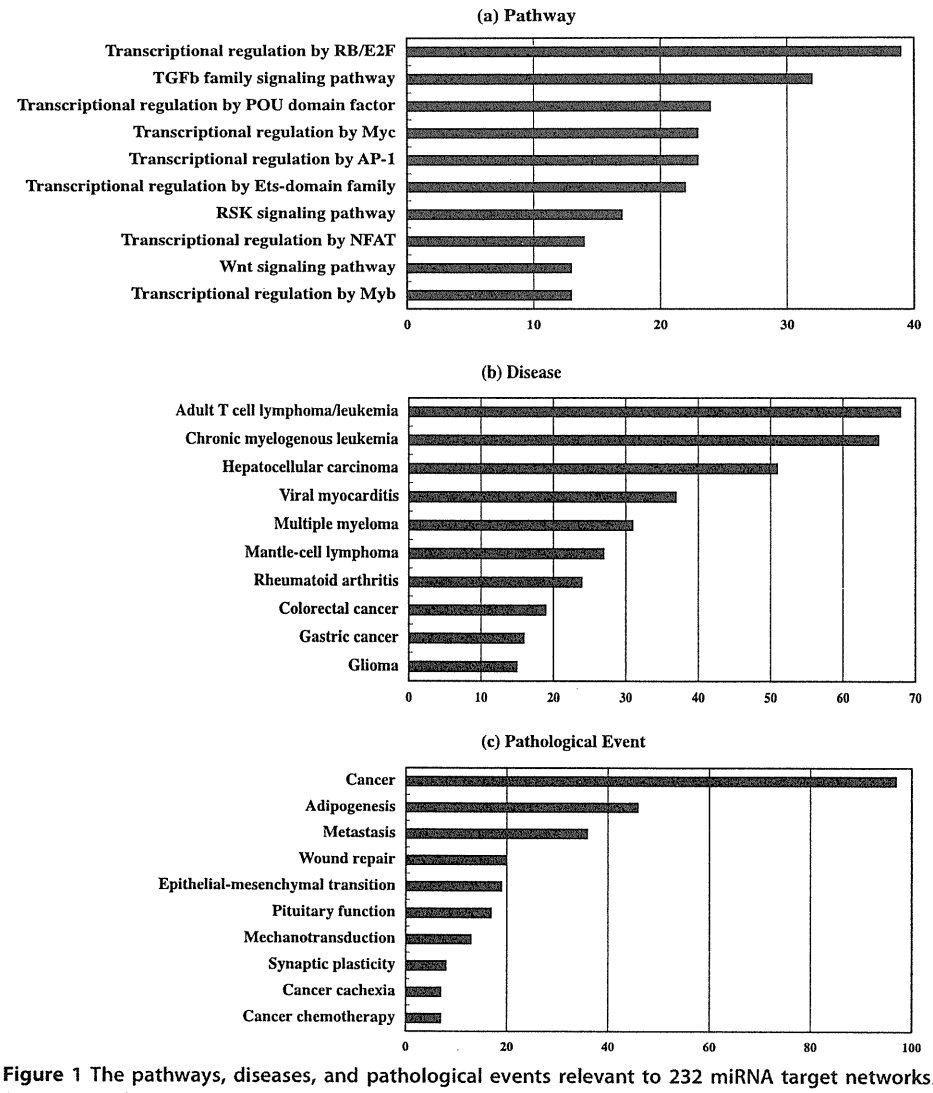

Figure 1 The pathways, diseases, and pathological events relevant to 232 miRNA target networks. Among 1,223 human miRNAs examined, Diana-microT 3.0 identified the set of reliable targets from 273 miRNAs. Among them, KeyMolnet extracted molecular networks from 232 miRNAs. The generated network was compared side by side with human canonical networks of the KeyMolnet library, composed of 430 pathways, 885 diseases, and 208 pathological events to identify the canonical network showing the most statistically significant contribution to the extracted network (see Table S1 for all the information). After top three pathways, diseases, and pathological events were individually totalized, the cumulated numbers of top 10 of **(a)** pathway, **(b)** disease, and **(c)** pathological event categories are expressed as a bar graph.

functionally-associated molecules in human cells. Therefore, it is highly important to obtain deeper insights into biological implications of miRNA target networks.

The protooncogene c-myb is a key transcription factor for normal development of hematopoietic cells. A recent study showed that miR-15a targets c-myb, while c-myb binds to the promoter of miR-15a, providing an autoregulatory feedback loop in human hematopoietic cells [17]. Consistent with this study, we found 'transcriptional regulation by myb' as the most relevant pathway to the miR-15a target network (the score = 602; the score p-value = 7.39E-182) (Figure 2 and Additional file 1). These observations propose a scenario that miR-15a synchronously downregulates both c-myb itself and downstream genes transcriptionally regulated by c-myb, resulting in

Table 1 The large-scale human microRNA target networks

MicroRNA	Number of Targets	Molecules in KeyMolnet Networks	Top Pathway	Score	p-Value	Top Disease	Score	p-Value	Top Pathological Event	Score	p-Value
hsa-let-7a	244	1022	Transcriptional regulation by p53	593	2.69E-179	Viral myocarditis	113	1.21E-34	Cancer	206	1.31E-62
hsa-let-7b	242	1016	Transcriptional regulation by p53	594	1.83E-179	Viral myocarditis	113	9.32E-35	Cancer	206	7.66E-63
hsa-let-7c	243	1020	Transcriptional regulation by p53	593	2.49E-179	Viral myocarditis	113	1.11E-34	Cancer	206	1.10E-62
hsa-let-7d	145	885	Transcriptional regulation by RB/E2F	836	2.18E-252	Chronic myelogenous leukemia	72	1.95E-22	Cancer	130	9.68E-40
hsa-let-7e	236	1111	Transcriptional regulation by p53	575	8.90E-174	Viral myocarditis	116	1.20E-35	Cancer	175	1.86E-53
hsa-let-7f	244	1022	Transcriptional regulation by p53	593	2.69E-179	Viral myocarditis	113	1.21E-34	Cancer	206	1.31E-62
hsa-let-7g	245	1022	Transcriptional regulation by p53	593	2.69E-179	Viral myocarditis	113	1.21E-34	Cancer	206	1.31E-62
hsa-let-7i	245	1022	Transcriptional regulation by p53	593	2.69E-179	Viral myocarditis	113	1.21E-34	Cancer	206	1.31E-62
hsa-miR-9	352	1115	Transcriptional regulation by PPARa	340	5.28E-103	Hepatocellular carcinoma	72	1.69E-22	Cancer	171	3.50E-52
hsa-miR-17	195	961	Transcriptional regulation by RB/E2F	971	3.27E-293	Chronic myelogenous leukemia	92	2.83E-28	Cancer	181	3.58E-55
hsa-miR-19a	226	1094	Transcriptional regulation by RB/E2F	760	2.10E-229	Chronic myelogenous leukemia	113	1.26E-34	Cancer	253	7.04E-77
hsa-miR-19b	225	1094	Transcriptional regulation by RB/E2F	760	2.10E-229	Chronic myelogenous leukemia	113	1.26E-34	Cancer	253	7.04E-77
hsa-miR-20a	165	1038	Transcriptional regulation by RB/E2F	856	1.64E-258	Chronic myelogenous leukemia	87	6.09E-27	Cancer	85	3.33E-26
hsa-miR-20b	198	981	Transcriptional regulation by RB/E2F	962	2.35E-290	Chronic myelogenous leukemia	98	3.39E-30	Cancer	183	6.98E-56
hsa-miR-26a	148	672	Transcriptional regulation by RB/E2F	919	1.76E-277	Chronic myelogenous leukemia	107	6.15E-33	Cancer	181	3.20E-55
hsa-miR-26b	148	672	Transcriptional regulation by RB/E2F	919	1.76E-277	Chronic myelogenous leukemia	107	6.15E-33	Cancer	181	3.20E-55
hsa-miR-27a	229	1192	Transcriptional regulation by CREB	1022	2.23E-308	Chronic myelogenous leukemia	95	1.96E-29	Cancer	194	3.05E-59
hsa-miR-27b	261	1337	Transcriptional regulation by CREB	1022	2.23E-308	Chronic myelogenous leukemia	94	4.51E-29	Cancer	211	4.11E-64
hsa-miR-29a	119	543	Transcriptional regulation by Ets-domain family	430	4.36E-130	Glioma	85	3.46E-26	Cancer	139	1.41E-42

Table 1 The large-scale human microRNA target networks *(Continued)*

hsa-miR-29b	118	578	Transcriptional regulation by Ets-domain family	422	1.15E-127	Glioma	82	1.55E-25	Cancer	146	1.44E-44
hsa-miR-29c	118	543	Transcriptional regulation by Ets-domain family	430	4.36E-130	Glioma	85	3.46E-26	Cancer	139	1.41E-42
hsa-miR-30a	455	1494	Transcriptional regulation by RB/E2F	777	9.43E-235	Chronic myelogenous leukemia	86	1.11E-26	Cancer	195	2.39E-59
hsa-miR-30b	455	1480	Transcriptional regulation by RB/E2F	781	1.08E-235	Chronic myelogenous leukemia	87	7.01E-27	Cancer	188	1.92E-57
hsa-miR-30c	454	1495	Transcriptional regulation by RB/E2F	778	6.13E-235	Chronic myelogenous leukemia	86	1.15E-26	Cancer	191	3.63E-58
hsa-miR-30d	452	1491	Transcriptional regulation by RB/E2F	778	7.28E-235	Chronic myelogenous leukemia	86	1.01E-26	Cancer	195	1.96E-59
hsa-miR-30e	455	1481	Transcriptional regulation by RB/E2F	780	1.29E-235	Chronic myelogenous leukemia	87	7.25E-27	Cancer	188	2.05E-57
hsa-miR-32	261	905	Transcriptional regulation by RB/E2F	842	2.74E-254	Gastric cancer	80	8.85E-25	Cancer	157	4.19E-48
hsa-miR-92a	219	642	Transcriptional regulation by MEF2	335	1.51E-101	Viral myocarditis	59	1.62E-18	Epithelial-mesenchymal transition	83	7.76E-26
hsa-miR-92b	258	701	Transcriptional regulation by MEF2	328	1.59E-99	Viral myocarditis	60	1.23E-18	Cancer	94	3.97E-29
hsa-miR-93	195	958	Transcriptional regulation by RB/E2F	972	2.37E-293	Chronic myelogenous leukemia	92	2.47E-28	Cancer	181	2.77E-55
hsa-miR-96	142	688	Transcriptional regulation by Ets-domain family	407	3.42E-123	Viral myocarditis	36	1.06E-11	Cancer	106	1.37E-32
hsa-miR-98	162	671	Transcriptional regulation by Myb	549	4.73E-166	Viral myocarditis	85	2.66E-26	Cancer	126	1.42E-38
hsa-miR-101	188	806	Transcriptional regulation by AP-1	492	1.10E-148	Hepatocellular carcinoma	70	6.40E-22	Cancer	127	4.26E-39
hsa-miR-106b	164	1028	Transcriptional regulation by RB/E2F	854	7.21E-258	Chronic myelogenous leukemia	87	5.48E-27	Cancer	85	2.93E-26
hsa-miR-124	285	1346	Transcriptional regulation by RB/E2F	756	3.57E-228	Chronic myelogenous leukemia	83	9.34E-26	Cancer	185	1.90E-56
hsa-miR-137	288	941	Transcriptional regulation by MITF family	339	1.19E-102	Adult T cell lymphoma/ leukemia	66	1.30E-20	Cancer	179	1.00E-54
hsa-miR-147	199	867	Transcriptional regulation by RB/E2F	805	4.06E-243	Chronic myelogenous leukemia	113	6.60E-35	Cancer	132	2.57E-40
hsa-miR-153	154	1019	Transcriptional regulation by Myb	507	2.35E-153	Multiple myeloma	60	6.44E-19	Cancer	174	4.31E-53

Table 1 The large-scale human microRNA target networks *(Continued)*

hsa-miR-218	155	830	Transcriptional regulation by AP-1	344	2.28E-104	Hepatocellular carcinoma	69	1.63E-21	Cancer	136	1.52E-41
hsa-miR-372	101	562	Transcriptional regulation by RB/E2F	1022	2.23E-308	Chronic myelogenous leukemia	85	1.90E-26	Cancer	144	2.75E-44
hsa-miR-429	123	634	Transcriptional regulation by RB/E2F	918	2.45E-277	Chronic myelogenous leukemia	76	1.71E-23	Cancer	130	5.28E-40
hsa-miR-495	156	601	Transcriptional regulation by Ets-domain family	431	2.14E-130	Rheumatoid arthritis	77	5.90E-24	Adipogenesis	79	1.32E-24
hsa-miR-506	394	1536	Transcriptional regulation by Ets-domain family	317	4.69E-96	Viral myocarditis	99	1.73E-30	Cancer	172	1.43E-52
hsa-miR-519a	281	1256	Transcriptional regulation by RB/E2F	811	5.32E-245	Chronic myelogenous leukemia	106	1.34E-32	Cancer	220	8.03E-67
hsa-miR-519b-3p	281	1256	Transcriptional regulation by RB/E2F	811	5.32E-245	Chronic myelogenous leukemia	106	1.34E-32	Cancer	220	8.03E-67
hsa-miR-519c-3p	281	1256	Transcriptional regulation by RB/E2F	811	5.32E-245	Chronic myelogenous leukemia	106	1.34E-32	Cancer	220	8.03E-67
hsa-miR-520a-3p	184	690	Transcriptional regulation by RB/E2F	1022	2.23E-308	Chronic myelogenous leukemia	94	6.95E-29	Cancer	146	1.12E-44
hsa-miR-520b	182	690	Transcriptional regulation by RB/E2F	1022	2.23E-308	Chronic myelogenous leukemia	94	6.95E-29	Cancer	146	1.12E-44
hsa-miR-520c-3p	182	690	Transcriptional regulation by RB/E2F	1022	2.23E-308	Chronic myelogenous leukemia	93	9.28E-29	Cancer	145	1.77E-44
hsa-miR-520d-3p	183	690	Transcriptional regulation by RB/E2F	1022	2.23E-308	Chronic myelogenous leukemia	94	6.95E-29	Cancer	146	1.12E-44
hsa-miR-520e	184	690	Transcriptional regulation by RB/E2F	1022	2.23E-308	Chronic myelogenous leukemia	94	6.95E-29	Cancer	146	1.12E-44
hsa-miR-603	252	1150	Transcriptional regulation by Ets-domain family	344	3.26E-104	Multiple myeloma	84	4.36E-26	Cancer	161	4.24E-49

Among 1,223 human miRNAs examined, Diana-microT 3.0 predicted reliable targets from 273 miRNAs. Among them, KeyMolnet extracted molecular networks from 232 miRNAs. The generated network was compared side by side with human canonical networks of the KeyMolnet library, composed of 430 pathways, 885 diseases, and 208 pathological events. The canonical pathways, diseases, and pathological events with the most statistically significant contribution to the extracted network are shown. The table contains only the large-scale miRNA target networks generated by importing targets greater than 100 per individual miRNA into KeyMolnet. See Additional file 1 for all the information on 232 miRNAs and their target networks.

efficient inactivation of the whole molecular network governed by the hub gene c-myb. These results suggest a collaborative regulation of gene expression at both transcriptional and posttranscriptional levels that involve coordinated regulation by miRNAs and transcription factors.

The retinoblastoma protein Rb/E2F pathway acts as a gatekeeper for G1/S transition in the cell cycle. The Rb/E2F-regulated G1 checkpoint control is often disrupted in cancer cells. A recent study showed that miR-106b is directly involved in posttranscriptional regulation of E2F1 [18]. E2F1 activates transcription of miR-106b, while miR-

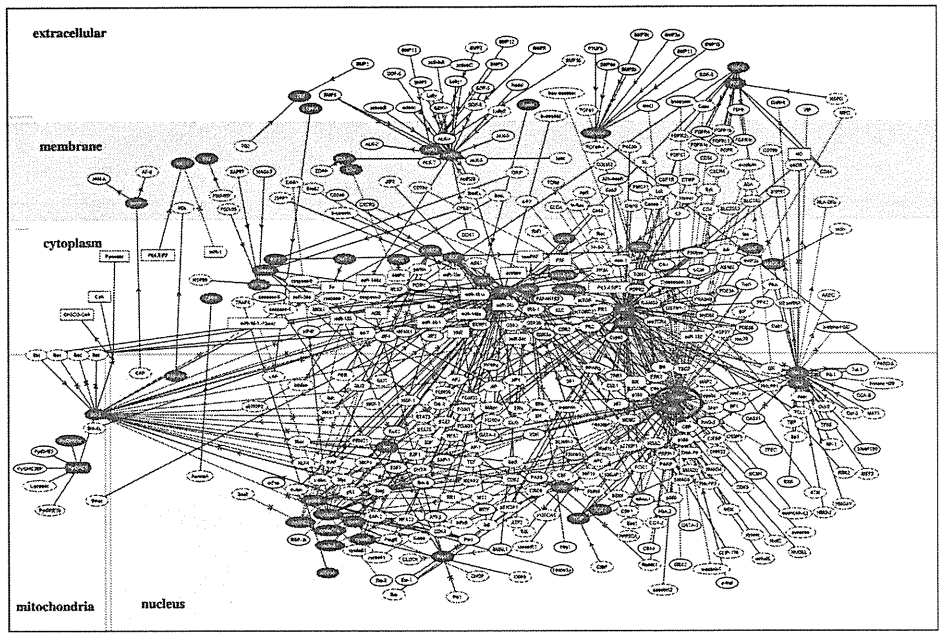

Figure 2 Molecular network of miR-15a targets. By the "neighboring" network-search algorithm, KeyMolnet illustrated a highly complex network of miR-15a targets that has the most statistically significant relationship with the pathway of 'transcriptional regulation by myb'. Red nodes represent miR-15a direct target molecules predicted by Diana-microT 3.0, whereas white nodes exhibit additional nodes extracted automatically from the core contents of KeyMolnet to establish molecular connections. The molecular relation is indicated by solid line with arrow (direct binding or activation), solid line with arrow and stop (direct inactivation), solid line without arrow (complex formation), dash line with arrow (transcriptional activation), and dash line with arrow and stop (transcriptional repression). The transcription factor myb is highlighted by a blue circle.

106b targets E2F1, serving as a miRNA-directed negative feedback loop in gastric cancer cells [18]. Supporting these findings, we identified 'transcriptional regulation by Rb/E2F' as the most relevant pathway to the miR-106b target network (the score = 854; the score p-value = 7.21E-258) (Figure 3, Table 1 and Additional file 1). The relationship between miR-106b and Rb/E2F would provide another example of coordinated regulation of gene expression by miRNAs and transcription factors.

We found 'transcriptional regulation by p53' as the most relevant pathway to the target network of all let-7 family members except for let-7d (Table 1). It is worthy to note that the tumor suppressor p53 regulates the expression of components of the miRNA-processing machinery, such as Drosha, DGCR8, Dicer, and TARBP2, all of which have p53-reponsive elements in their promoters [19]. Furthermore, Dicer and TARBP2, along with p53, serve as a target of the let-7 family miRNAs, suggesting a close link between p53 and let-7 in miRNA biogenesis [19]. The expression of let-7 family members was greatly reduced in certain cancer cells [20].

The micropthalmia associated transcription factor (MITF), a basic helix-loop-helix zipper (bHLH-Zip) transcription factor, acts as not only a master regulator of melanocyte differentiation but also an oncogene promoting survival of melanoma. Recent studies indicate that MITF is a direct target of both miR-137 and miR-148b [21,22]. Again, we identified 'transcriptional regulation by MITF family' as the most relevant pathway to both miR-137 (the score = 339; the score p-value = 1.19E-102) and miR-

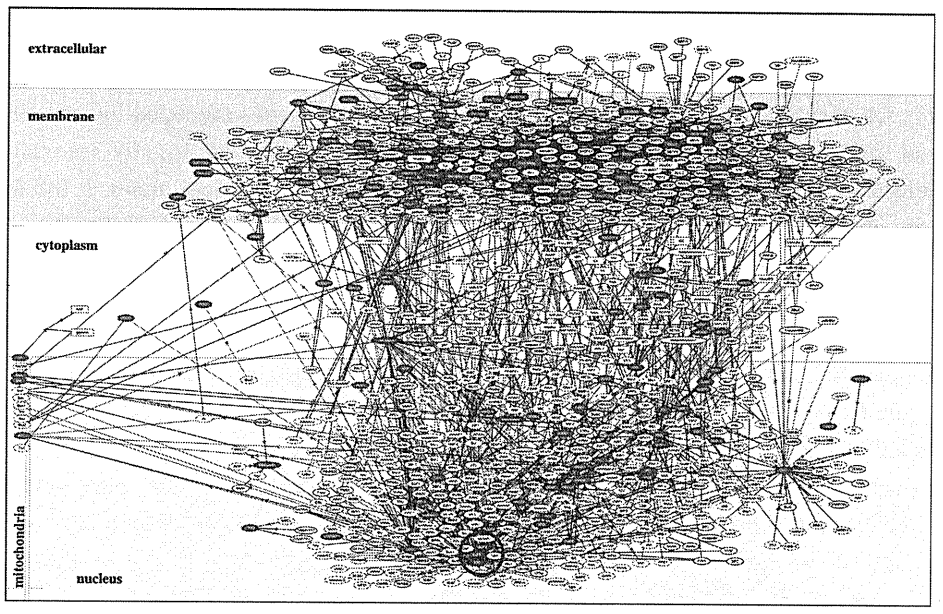

Figure 3 Molecular network of miR-106b targets. By the "neighboring" network-search algorithm, KeyMolnet illustrated a highly complex network of miR-106b targets that has the most statistically significant relationship with the pathway of 'transcriptional regulation by Rb/E2F'. Red nodes represent miR-106b direct target molecules predicted by Diana-microT 3.0, whereas white nodes exhibit additional nodes extracted automatically from the core contents of KeyMolnet to establish molecular connections. The molecular relation is indicated by solid line with arrow (direct binding or activation), solid line with arrow and stop (direct inactivation), solid line without arrow (complex formation), dash line with arrow (transcriptional activation), and dash line with arrow and stop (transcriptional repression). The transcription factor E2F is highlighted by a blue circle.

148b (the score = 40; the score p-value = 3.91E-142) target networks (Table 1 and Additional file 1).

Cellular responsiveness to glucocorticoids (GCs) is regulated by the delicate balance of the glucocorticoid receptor (GR) protein, GR coactivators and corepressors, GR splice variants and isoforms, and regulators of GR retrograde transport to the nucleus. A recent study showed that miR-18a targets the GR protein, and thereby inhibits GR-mediated biological events in neuronal cells [23]. Consistent with this, we found 'transcriptional regulation by GR' as the most relevant pathway to the miR-18a target network (the score = 1022; the score p-value = 2.23E-308) (Additional file 1).

Zinc finger transcription factors ZEB1 and ZEB2 act as a transcriptional repressor of E-cadherin. A recent study showed that the expression of miR-200b, which targets both ZEB1 and ZEB2, was downregulated in the cells that undergo TGF-beta-induced epithelial to mesenchymal transition (EMT), and was lost in invasive breast cancer cells [24]. We identified 'transcriptional regulation by ZEB' as the third-rank significant pathway (the score = 155; the score p-value = 1.88E-47) and 'EMT' as the third-rank significant pathological event relevant to the miR-200b target network (the score = 61; the score p-value = 4.15E-19) (Additional file 1).

Discussion

In general, a single miRNA concurrently downregulates hundreds of target mRNAs by binding to the corresponding 3'UTR of mRNA via either perfect or imperfect sequence complementarity [3]. Such fuzzy mRNA-miRNA interactions result in the redundancy

of miRNA-recognized targets. By targeting multiple transcripts and affecting expression of numerous proteins at one time, miRNAs regulate a wide range of cellular functions, such as development, differentiation, proliferation, apoptosis and metabolism. Therefore, we have the question whether a set of miRNA target genes regulated by an individual miRNA generally constitute the biological network of functionally-associated molecules or simply reflect a random set of functionally-independent genes. If the former is the case, what kind of biological networks does the human microRNAome most actively regulates?

To address these questions, first we identified the set of credible target genes for all individual human miRNAs by using the Diana-microT 3.0 program. Then, we investigated miRNA target networks by applying them to KeyMolnet, a bioinformatics tool for analyzing molecular interactions on the comprehensive knowledgebase. Diana-microT 3.0 identified highly reliable targets from 273 miRNAs out of 1,223 all human miRNAs. Previous studies showed that the list of predicted targets for each miRNA varies among different miRNA target prediction programs armed with distinct algorithms, such as TargetScan 5.1 http://www.targetscan.org, PicTar (pictar.mdc-berlin.de), miRanda http://www.microrna.org and Diana-microT 3.0 [25]. Therefore, miRNA target networks are to some extent flexible, depending on the target prediction program employed. Among the programs described above, we have chosen Diana-microT 3.0 because of the highest ratio of correctly predicted targets over other prediction tools and the simplicity of setting a cut-off point for detection of reliable miRNA-target interactions based on the miTG score [11].

Here we found that highly reliable targets of substantial numbers of human miRNAs actually constructed biologically meaningful molecular networks. These observations strongly supported the theoretical view that miRNA target genes regulated by an individual miRNA in the whole human microRNAome generally constitute the biological network of functionally-associated molecules. A recent study showed that interacting proteins in the human PPI network tend to share restricted miRNA target-site types than random pairs, being consistent with our observations [26].

We also found that there exists a coordinated regulation of gene expression at the transcriptional level by transcription factors and at the posttranscriptional level by miRNAs in miRNA target networks. Recently, Cui et al. investigated the relationship between miRNA and transcription factors in gene regulation [27]. Importantly, they found that the genes with more transcription factor-binding sites have a higher probability of being targeted by miRNAs and have more miRNA-binding sites.

A recent study by miRNA expression profiling of thousands of human tissue samples revealed that diverse miRNAs constitute a complex network composed of coordinately regulated miRNA subnetworks in both normal and cancer tissues, and they are often disorganized in solid tumors and leukemias [28]. During carcinogenesis, various miRNAs play a central role, acting as either oncogenes named oncomir or tumor suppressors termed anti-oncomir, by targeting key molecules involved in apoptosis, cell cycle, cell adhesion and migration, chromosome stability, and DNA repair [5]. Many miRNA gene loci are clustered in cancer-associated genomic regions [29]. Furthermore, miRNA expression signatures well discriminate different types of cancers with distinct clinical prognoses [30]. In the present study, KeyMolnet analysis of miRNA target networks showed that the most relevant pathological event is 'cancer', when top three

pathological events were overall cumulated. Furthermore, the highly relevant diseases include 'adult T cell lymphoma/leukemia', 'chronic myelogenous leukemia', and 'hepatocellular carcinoma'. These observations suggest that the human microRNAome plays a more specialized role in regulation of oncogenesis. Therefore, the miRNA-based therapy directed to targeting multiple cancer-associated pathways simultaneously might serve as the most effective approach to suppressing the oncogenic potential of a wide range of cancers.

Conclusion

The reliable targets predicted by Diana microT 3.0 derived from approximately 20% of all human miRNAs constructed biologically meaningful molecular networks by KeyMolnet. These observations support the view that miRNA target genes regulated by an individual miRNA in the whole human microRNAome generally constitute the biological network of functionally-associated molecules. In the human miRNA target networks, the most relevant pathway is transcriptional regulation by transcription factors RB/E2F, the disease is adult T cell lymphoma/leukemia, and the pathological event is cancer. In miRNA target networks, there exists a coordinated regulation of gene expression at the transcriptional level by transcription factors and at the posttranscriptional level by miRNAs.

Additional material

Additional file 1: KeyMolnet identifies microRNA target networks in 232 human miRNAs. The prediction of target genes of individual miRNA was performed by Diana-microT 3.0. Entrez Gene IDs of miRNA target genes were uploaded onto KeyMolnet. The generated network was compared side by side with human canonical networks composed of 430 pathways, 885 diseases, and 208 pathological events of the KeyMolnet library. Top-three pathways, diseases, and pathological events with the statistically significant contribution to the extracted network are shown.

Acknowledgements
This work was supported by grants from the Research on Intractable Diseases (H22-Nanchi-Ippan-136), the Ministry of Health, Labour and Welfare (MHLW), Japan and the High-Tech Research Center Project (S0801043) and the Grant-in-Aid (C22500322), the Ministry of Education, Culture, Sports, Science and Technology (MEXT), Japan.

Authors' contributions
JS designed the methods, analyzed the data, and drafted the manuscript. HT helped the data analysis. All authors have read and approved the final manuscript.

Competing interests
The authors declare that they have no competing interests.

Received: 13 October 2010 Accepted: 17 June 2011 Published: 17 June 2011

References

1. Guo H, Ingolia NT, Weissman JS, Bartel DP: **Mammalian microRNAs predominantly act to decrease target mRNA levels.** *Nature* 2010, 466:835-40.
2. Bartel DP: **MicroRNAs: target recognition and regulatory functions.** *Cell* 2009, 136:215-33.
3. Selbach M, Schwanhäusser B, Thierfelder N, Fang Z, Khanin R, Rajewsky N: **Widespread changes in protein synthesis induced by microRNAs.** *Nature* 2008, 455:58-63.
4. Friedman RC, Farh KK, Burge CB, Bartel DP: **Most mammalian mRNAs are conserved targets of microRNAs.** *Genome Res* 2009, 19:92-105.
5. Garzon R, Marcucci G, Croce CM: **Targeting microRNAs in cancer: rationale, strategies and challenges.** *Nat Rev Drug Discov* 2010, 9:775-89.
6. Shioya M, Obayashi S, Tabunoki H, Arima K, Saito Y, Ishida T, Satoh J: **Aberrant microRNA expression in the brains of neurodegenerative diseases: miR-29a decreased in Alzheimer disease brains targets neurone navigator 3.** *Neuropathol Appl Neurobiol* 2010, 36:320-30.
7. Viswanathan GA, Seto J, Patil S, Nudelman G, Sealfon SC: **Getting started in biological pathway construction and analysis.** *PLoS Comput Biol* 2008, 4:e16.

8. Kitano H: **A robustness-based approach to systems-oriented drug design.** *Nat Rev Drug Discov* 2007, **6**:202-10.
9. Albert R, Jeong H, Barabasi AL: **Error and attack tolerance of complex networks.** *Nature* 2000, **406**:378-82.
10. Hsu CW, Juan HF, Huang HC: **Characterization of microRNA-regulated protein-protein interaction network.** *Proteomics* 2008, **8**:1975-79.
11. Maragkakis M, Alexiou P, Papadopoulos GL, Reczko M, Dalamagas T, Giannopoulos G, Goumas G, Koukis E, Kourtis K, Simossis VA, Sethupathy P, Vergoulis T, Koziris N, Sellis T, Tsanakas P, Hatzigeorgiou AG: **Accurate microRNA target prediction correlates with protein repression levels.** *BMC Bioinformatics* 2009, **10**:295.
12. Huang da W, Sherman BT, Lempicki RA: **Systematic and integrative analysis of large gene lists using DAVID bioinformatics resources.** *Nat Protoc* 2009, **4**:44-57.
13. Sato H, Ishida S, Toda K, Matsuda R, Hayashi Y, Shigetaka M, Fukuda M, Wakamatsu Y, Itai A: **New approaches to mechanism analysis for drug discovery using DNA microarray data combined with KeyMolnet.** *Curr Drug Discov Technol* 2005, **2**:89-98.
14. Satoh JI, Tabunoki H, Yamamura T: **Molecular network of the comprehensive multiple sclerosis brain-lesion proteome.** *Mult Scler* 2009, **15**:531-41.
15. Satoh J, Tabunoki H, Arima K: **Molecular network analysis suggests aberrant CREB-mediated gene regulation in the Alzheimer disease hippocampus.** *Dis Markers* 2009, **27**:239-52.
16. Boyle EI, Weng S, Gollub J, Jin H, Botstein D, Cherry JM, Sherlock G: **GO::TermFinder–open source software for accessing Gene Ontology information and finding significantly enriched Gene Ontology terms associated with a list of genes.** *Bioinformatics* 2004, **20**:3710-15.
17. Zhao H, Kalota A, Jin S, Gewirtz AM: **The c-myb proto-oncogene and microRNA-15a comprise an active autoregulatory feedback loop in human hematopoietic cells.** *Blood* 2009, **113**:505-16.
18. Petrocca F, Visone R, Onelli MR, Shah MH, Nicoloso MS, de Martino I, Iliopoulos D, Pilozzi E, Liu CG, Negrini M, Cavazzini L, Volinia S, Alder H, Ruco LP, Baldassarre G, Croce CM, Vecchione A: **E2F1-regulated microRNAs impair TGFβ-dependent cell-cycle arrest and apoptosis in gastric cancer.** *Cancer Cell* 2008, **13**:272-86.
19. Boominathan L: **The tumor suppressors p53, p63, and p73 are regulators of microRNA processing complex.** *PLoS One* 2010, **5**:e10615.
20. Takamizawa J, Konishi H, Yanagisawa K, Tomida S, Osada H, Endoh H, Harano T, Yatabe Y, Nagino M, Nimura Y, Mitsudomi T, Takahashi T: **Reduced expression of the let-7 microRNAs in human lung cancers in association with shortened postoperative survival.** *Cancer Res* 2004, **64**:3753-56.
21. Bemis LT, Chen R, Amato CM, Classen EH, Robinson SE, Coffey DG, Erickson PF, Shellman YG, Robinson WA: **MicroRNA-137 targets microphthalmia-associated transcription factor in melanoma cell lines.** *Cancer Res* 2008, **68**:1362-68.
22. Haflidadóttir BS, Bergsteinsdóttir K, Praetorius C, Steingrímsson E: **miR-148 regulates Mitf in melanoma cells.** *PLoS One* 2010, **5**:e11574.
23. Vreugdenhil E, Verissimo CS, Mariman R, Kamphorst JT, Barbosa JS, Zweers T, Champagne DL, Schouten T, Meijer OC, de Kloet ER, Fitzsimons CP: **MicroRNA 18 and 124a down-regulate the glucocorticoid receptor: implications for glucocorticoid responsiveness in the brain.** *Endocrinology* 2009, **150**:2220-28.
24. Gregory PA, Bert AG, Paterson EL, Barry SC, Tsykin A, Farshid G, Vadas MA, Khew-Goodall Y, Goodall GJ: **The miR-200 family and miR-205 regulate epithelial to mesenchymal transition by targeting ZEB1 and SIP1.** *Nat Cell Biol* 2008, **10**:593-601.
25. Boross G, Orosz K, Farkas I: **Human microRNAs co-silence in well-separated groups and have different predicted essentialities.** *Bioinformatics* 2009, **25**:1063-69.
26. Liang H, Li WH: **MicroRNA regulation of human protein protein interaction network.** *RNA* 2007, **13**:1402-8.
27. Cui Q, Yu Z, Pan Y, Purisima EO, Wang E: **MicroRNAs preferentially target the genes with high transcriptional regulation complexity.** *Biochem Biophys Res Commun* 2007, **352**:733-38.
28. Volinia S, Galasso M, Costinean S, Tagliavini L, Gamberoni G, Drusco A, Marchesini J, Mascellani N, Sana ME, Abu Jarour R, Desponts C, Teitell M, Baffa R, Aqeilan R, Iorio MV, Taccioli C, Garzon R, Di Leva G, Fabbri M, Catozzi M, Previati M, Ambs S, Palumbo T, Garofalo M, Veronese A, Bottoni A, Gasparini P, Harris CC, Visone R, Pekarsky Y, de la Chapelle A, Bloomston M, Dillhoff M, Rassenti LZ, Kipps TJ, Huebner K, Pichiorri F, Lenze D, Cairo S, Buendia MA, Pineau P, Dejean A, Zanesi N, Rossi S, Calin GA, Liu CG, Palatini J, Negrini M, Vecchione A, Rosenberg A, Croce CM: **Reprogramming of miRNA networks in cancer and leukemia.** *Genome Res* 2010, **20**:589-99.
29. Calin GA, Sevignani C, Dumitru CD, Hyslop T, Noch E, Yendamuri S, Shimizu M, Rattan S, Bullrich F, Negrini M, Croce CM: **Human microRNA genes are frequently located at fragile sites and genomic regions involved in cancers.** *Proc Natl Acad Sci USA* 2004, **101**:2999-3004.
30. Lu J, Getz G, Miska EA, Alvarez-Saavedra E, Lamb J, Peck D, Sweet-Cordero A, Ebert BL, Mak RH, Ferrando AA, Downing JR, Jacks T, Horvitz HR, Golub TR: **MicroRNA expression profiles classify human cancers.** *Nature* 2005, **435**:834-38.

doi:10.1186/1756-0381-4-17
Cite this article as: Satoh and Tabunoki: **Comprehensive analysis of human microRNA target networks.** *BioData Mining* 2011 **4**:17.

多発性硬化症・視神経脊髄炎に対する免疫療法

Immunotherapy for Multiple Sclerosis and Neuromyelitis Optica

荒浪利昌
Toshimasa Aranami

多発性硬化症（MS）は，中枢神経系に広く病変が多発し，髄鞘抗原特異的T細胞やB細胞が介在する自己免疫疾患であると考えられており，病原性細胞としてTh1細胞とともにTh17細胞が注目されている．一方，視神経と脊髄が冒される視神経脊髄炎（NMO）には，血中にアクアポリン4に対する自己抗体（抗AQP4抗体）が存在し，病態形成に関与すると考えられている．MS治療の中心であるIFN-βは，Th1細胞の働きが亢進している病態では効果が期待されるが，Th17細胞が優位な状況では無効である可能性がある．NMOに対する新たな免疫療法として，抗CD20抗体などによる液性免疫を標的とする治療の有効性が示唆されている．

key words　多発性硬化症，視神経脊髄炎，免疫療法

はじめに

多発性硬化症（multiple sclerosis；MS）は，髄鞘抗原特異的なT細胞やB細胞が髄鞘を傷害することにより脱髄病変が生じる中枢神経系の自己免疫疾患であると考えられている．病変は中枢神経系に広く分布し，再発・寛解を繰り返し，視力低下や運動麻痺などの症状が長期にわたる．一方，視神経脊髄炎（neuromyelitis optica；NMO）は，病変が比較的視神経と脊髄に限局している．以前はMSの一病型と考えられていたが，患者末梢血中にアクアポリン4（AQP4）という水チャネル分子に対する自己抗体（抗AQP4抗体）が存在することが発見されて以来[1]，MSとは異なる病態であるとの考えが優勢である．本稿では，MSとNMOの免疫病態およびそれぞれに対する免疫療法の進歩を概説する．

Ⅰ　MSおよびNMOの病態

ヘルパーT（Th）細胞は活性化とともに，特定のサイトカイン産生細胞へと分化するが，従来より自己免疫疾患においてはTh1細胞の過剰な働きが関与するとの考えが優勢であった．しかし近年，インターロイキン（IL）-17を産生するT細胞（Th17細胞）が新たなTh細胞分画として提唱され，MSやその動物モデルである実験的自己免疫性脳脊髄炎（experimental autoimmune encephalomyelitis；EAE）への関与が示唆されている[2]．当初，Th17細胞は，Th1細胞とは異なるT細胞分画であり，EAE病態においてTh1細胞よりも高い病原性を有する分画として提唱されたが，近年IL-17を産生しているT細胞が，後にIFN-γ産生細胞へと変化すること，いわゆる可塑性（plasticity）を有することが示唆されている[3]．また，MSの末梢血や髄液においてもIL-17産生細胞の増加が報告されている[4]．その一方で，Th1およびTh17細胞の分化あるいは病原性の獲得を抑制することが期待されたIL-12とIL-23の中和抗体は，乾癬には有効であったが，MSにおいては再発抑制効果を認めなかった[5]．以上から，MS病態におけるTh1細胞およびTh17細胞の重要性については，いまだ結論は得られていない．また，MS病態においては，$CD4^+Foxp3^+$制御性T細胞（Treg）などのTreg機能の減弱も報告されており[6]，病原性細胞とTregのバランスにより，再発寛解型MSの病態が形成される可能性がある．

一方，NMOの免疫病態の特徴の1つは抗AQP4抗体の存在である．AQP4分子は中枢神経系グリア細胞アストロサイトの足突起などに特に豊富に存在している．NMO患者血清はアストロサイトを補体依存性に傷害し，EAEを誘導したマウスにNMO患者IgGを投与したところ，NMOに酷似した病理像が得られ，臨床症状も増悪したことから，抗AQP4抗体はNMO病態マーカーと言うだけでなく，病態形成に深く関わっているという考え方が有力である．当研究部の千原らは，NMOとMS，健常者の末梢血B細胞分画の頻度を比較し，他の2群と比べ，NMOにおいて形質芽細胞（プラズマブラスト）が有意に増加していることを見いだした．

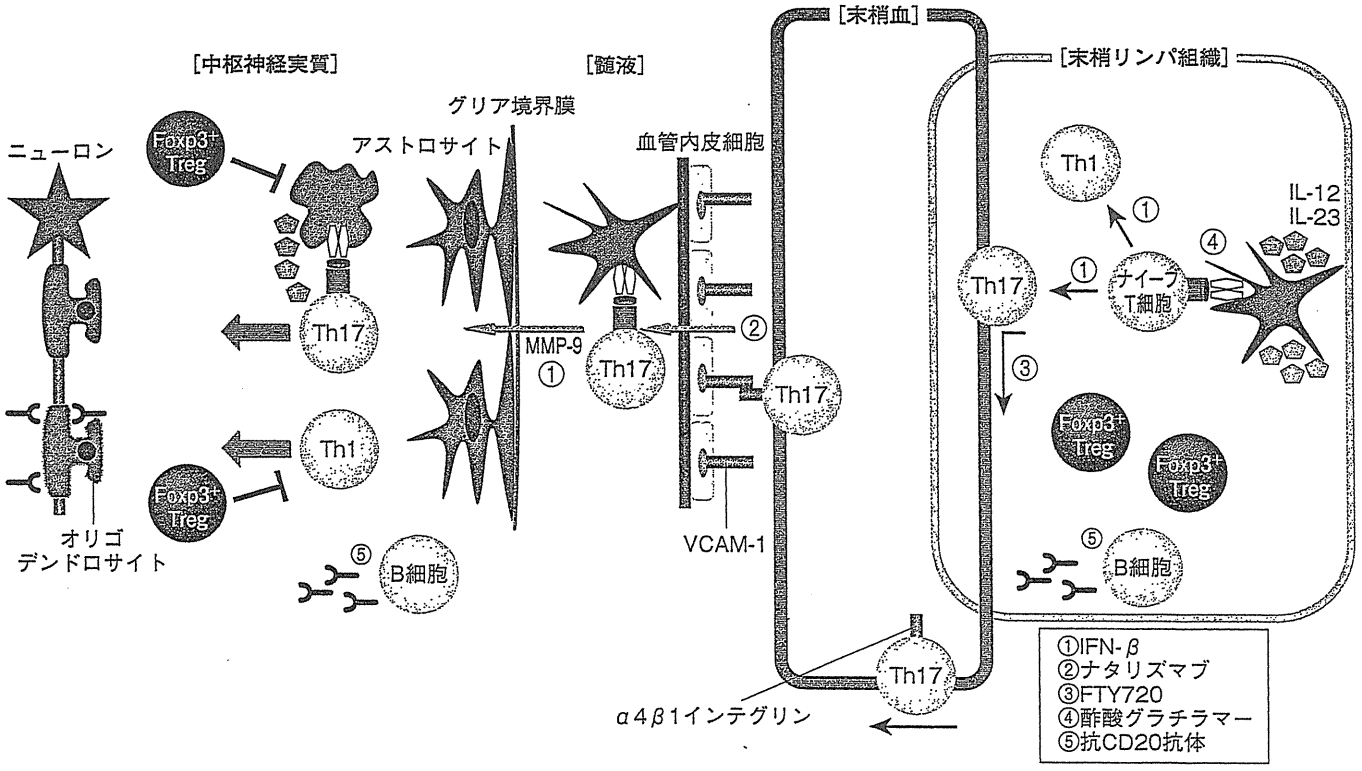

■図1 MS病態と免疫療法
MS病態への関与が示唆される病原性細胞およびTregと免疫療法の想定される作用点(①～⑤)を示す.

さらに,プラズマブラストが末梢血中の主たる抗AQP4抗体産生細胞であり,プラズマブラストの生存および抗AQP4抗体産生にIL-6が重要である可能性を示した[7].また,脳病変がほとんどなく,脊髄と視神経のみが選択的に冒されるMSが本邦を含むアジア諸国に多く,以前はOSMS(opticospinal MS)と呼ばれていたが,OSMSの30～60%は抗AQP4抗体陽性であることが明らかとなり,その病態形成機構はNMOと類似していると考えられている.そのOSMSの髄液においてはIL-17, IL-8, G-CSF(granulocyte colony-stimulating factor)といったIL-17ファミリーとそれにより誘導されるサイトカインの増加が認められる[8].また,NMOの髄液ではマウスのTh17細胞分化に重要なサイトカインであるIL-6も増加している.これらの報告から,NMOの病態形成に液性免疫とともにTh17細胞やIL-6が関与している可能性が示唆される.

Ⅱ MSとNMOの免疫療法

MSおよびNMOの急性増悪時の治療法としては,メチルプレドニゾロンなどのステロイド大量点滴静注療法(パルス療法)や血漿交換療法が用いられる.それとともに,MSおよびNMOの治療においては,再発を予防する治療が長期的な神経機能的予後への影響を考えるうえで最も重要である.IFN-βは再発寛解型MSの再発予防療法として最も広く用いられている.それとともにMS患者の10～50%がIFN-βノンレスポンダー(無効群)であると報告されている.IFN-βの効果発現機構として,Th1細胞やTh17細胞への分化の抑制,あるいは炎症性細胞浸潤に重要なMMP-9(matrix metalloproteinase-9)の抑制など,様々な効果が指摘されている.近年,MS病態におけるIFN-βの治療効果発現機構について新たな知見があった.Axtellらは,髄鞘抗原特異的Th1細胞で誘導したEAEにはIFN-βが有効であり,逆に髄鞘抗原特異的Th17細胞で誘導したEAEはIFN-β投与により症状の増悪が見られることを報告した.Th1細胞を移入して誘導したEAEでは,IFN-β投与により脾臓でのIFN-γ産生の減少と,抑制性サイトカインIL-10産生の著明な増加が認められた.このようなIL-10産生亢進はIFN-γノックアウトマウスでは観察されなかったことから,IFN-βが有効性を発揮するためにはIFN-γシグナルが必要と考えられ

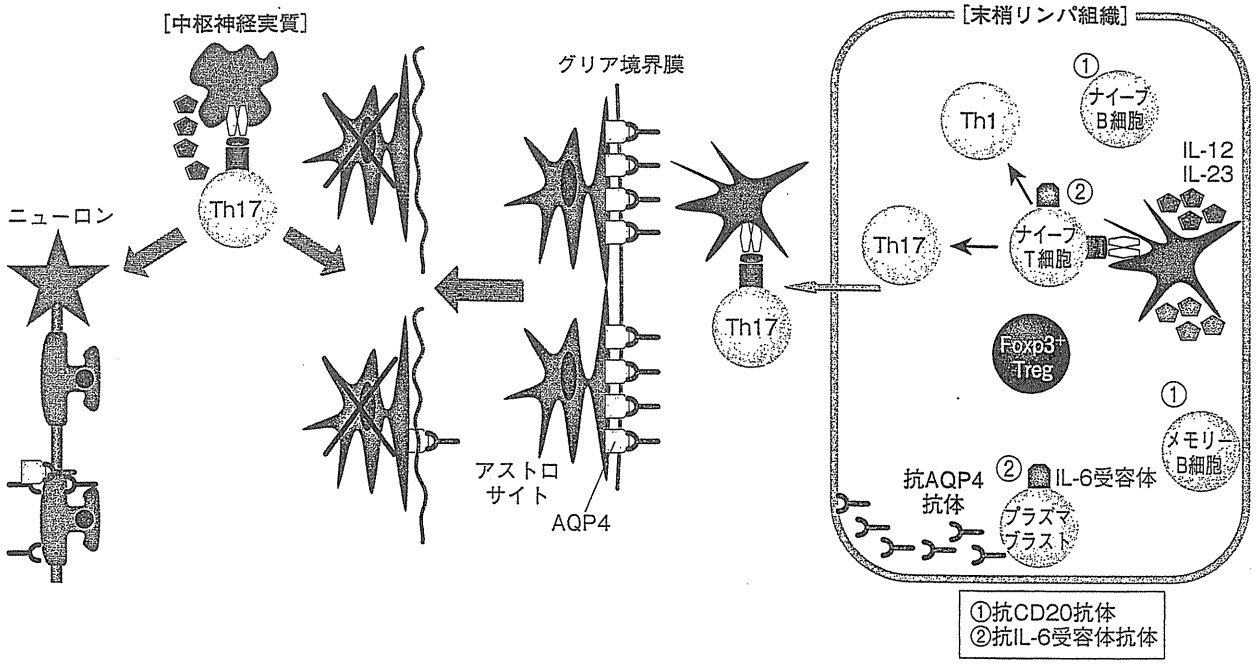

■図2 NMO病態と免疫療法

NMO病態への関与が示唆される病原性細胞およびTregとステロイド以外の免疫療法の想定される作用点(①～②)を示す.

た. 一方, Th17介在性EAEでは, IFN-β投与により脾臓でのIL-17産生は低下するが, IL-10産生に変化がなく, 脊髄でIL-17産生細胞がむしろ増加していたことから, IFN-γ産生の亢進がなければIFN-βによるIL-10産生誘導が生じず, 治療効果が見られないと考えられた. さらに, IFN-βノンレスポンダー中には, 治療前の血清中IL-17FとIFN-β濃度がレスポンダー(有効群)と比べて高い一群が存在し, マウスの実験系と同じく, Th17に偏倚(へんい)している状態では, IFN-β治療が無効であることが示唆された[9]. このように, MSの病態にはTh1に偏倚している状態とTh17に偏倚している状態が存在する可能性がある. 前者にはIFN-β治療が有効であるが, 後者ではむしろ病態を悪化させてしまう可能性があり, 検討が必要である.

MSの再発抑制療法としては, その他にも各種免疫抑制剤のほか, MS病態に即した免疫修飾薬が欧米を中心に用いられている. (1) 中枢神経系への免疫細胞の遊走を抑制する薬剤. (2) 自己反応性T細胞による髄鞘抗原の認識を阻害する薬剤. (3) 生体よりB細胞を除去する薬剤, などである.

(1) としては, ナタリズマブやFTY720がある. ナタリズマブはヒト化抗α4インテグリンモノクローナル抗体であり, 免疫系細胞に広く発現するα4β1インテグリンとVCAM-1 (vascular cell adhesion molecule-1) という接着分子の結合を阻害する働きがあり, 中枢神経系への炎症性細胞浸潤を阻害する機能を有する. MSの再発率を有意に低下させ, 欧米で再発寛解型MSの治療薬として使用されている. FTY720は, リンパ節や二次リンパ組織からのリンパ球の流出に必要なシグナルを阻害する新規化合物である. リンパ節からのリンパ球の流出には, スフィンゴシン1リン酸(S1P)がリンパ球上のS1P受容体に結合することが必要だが, FTY720は体内でリン酸化された後, S1P1受容体にアゴニストとして結合する. これによりS1P1受容体の細胞内へのinternalizationを誘導し, 結果としてS1Pに結合できるS1P1受容体数が減少し, リンパ球はS1P不応性となる. その結果, T細胞はリンパ節に留められることになり, 神経組織に浸潤するリンパ球が減少し, 炎症も抑制されると考えられる[10].

(2) としては酢酸グラチラマー(copolymer-1)がある. これは髄鞘タンパク質の1つであるミエリン塩基性タンパク質(myelin basic protein; MBP)と同じ頻度で混合された4種類のアミノ酸のランダムポリマーである. 酢酸グラチラマーはマウスおよびヒトの各種MHCクラスII分子に高いアフィニティーで結合することにより, MBPなどの髄鞘抗原がクラスII分子に結合することを競合的に阻害する.

(3) は抗CD20抗体であり, 生体よりB細胞を除去することで, やはりMSの再発率を有意に低下させることが示され

ている（図1）．

NMOの免疫療法に関して，MSとの違いはIFN-βに対する反応性である．NMO患者へのIFN-β治療において，かえって重症化した例が報告されたため，現在ではNMOと判定されれば，IFN-βは使用しない．IFN-βがNMOに対して無効である原因は不明であるが，IFN-β投与患者において，血清中BAFF（B cell-activating factor belonging to the TNF family）濃度が上昇することが報告されている．BAFFはB細胞生存や分化を促進する因子として重要なため，NMOにおいては抗AQP4抗体産生など液性免疫を刺激して，症状の悪化を引き起こす可能性が考えられる[11]．NMOの再発抑制療法としては，現在，経口ステロイド剤が中心であるが，MS同様，抗CD20抗体によるB細胞除去療法が有効であると報告されている．これは，NMO病態における液性免疫の重要性と符合する結果である．また，当研究部では現在，前記の研究結果に基づき，NMOに対する抗IL-6受容体抗体療法の臨床研究を計画している（図2）．

おわりに

MSにはIFN-βが有効な一群と無効な一群が存在し，後者にはTh17細胞やIFN-βが病態形成に関与している可能性がある．また，NMOにおいてもTh17細胞と液性免疫の重要性が示唆されており，やはりIFN-βは無効である可能性が高い．以上より，MS，NMOの免疫療法においては，個々の患者における病態機序を検討したうえで，治療法を選択することが重要であると考えられる．

PROFILE 荒浪利昌
■ 国立精神・神経医療研究センター 神経研究所
■ E-mail：aranami@ncnp.go.jp
1993年北海道大学医学部卒業．北海道大学大学院免疫科学研究所にて基礎免疫学を学ぶ．卒業後，国立精神・神経センター神経研究所免疫研究部研究員として多発性硬化症の病態解析研究に従事．2006年より同研究部室長．

文献

1) Lennon VA, et al: Lancet (2004) 364: 2106-2112
2) Diveu C, et al: Curr Opin Immunol (2008) 20: 663-668
3) Hirota K, et al: Nat Immunol (2011) 12: 255-263
4) Durelli L, et al: Ann Neurol (2009) 65: 499-509
5) Segal BM, et al: Lancet Neurol (2008) 7: 796-804
6) Dominguez-Villar M, et al: Nat Med (2011) 17: 673-675
7) Chihara N, et al: Proc Natl Acad Sci USA (2011) 108: 3701-3706
8) Ishizu T, et al: Brain (2005) 128: 988-1002
9) Axtell RC, et al: Nat Med (2010) 16: 406-412
10) Matloubian M, et al: Nature (2004) 427: 355-360
11) Krumbholz M, et al: Brain (2008) 131: 1455-1463